

# The Inverted Flight Optimization of the Genetic Algorithm to Hyper boost Vehicle Trajectory

Umakant Bhaskarrao Gohatre<sup>1</sup>, Dr. C. Ram Singla<sup>2</sup>

<sup>1,2</sup> Department of Electronics and Communication Engineering, Madhav University, Sirohi, India

## Abstract:

*Hypersonic interception in close space is a major challenge because of the unpredictable trajectory of the target, requiring trajectory cluster interceptors to cover the forecast area and the optimum ability to modify the trajectory in order to update the predicted midcourse impact location (PIP) consistently. Based on the next optimum theory of control is proposed a new mid-course optimum trajectory cluster generation and trajectory modification algorithm. Firstly, the problem of optimizing the midcourse trajectory; the conditions necessary to optimize control and the constraints on transversely are given. Secondly, with the description of the Nearby Optimum Trajectory Existence (NOTET), An inverted flight management approach is implemented to identify the best way in which a hypersonic missile dive can be entered. This article examines the fighting scene in which the hypersonic missile attacks the target. In particular, the hypersonic missile is a maneuvering form known as inverted flight. An optimal path is designed to minimize the attachment time with regard to angle, dynamic pressure, heat transfer speed and normal overload. In addition, inverted flight in contrast simulation is better performed than normal flight.*

**Keyword** - Aircraft Control, Optimal Control, Optimisation Position Control, Trajectory control, Mathematical Model, Prediction

## I. INTRODUCTION

Hypersonic cars are divided into three typical categories: re-entry gliding, air traffic cruise and rocket-driven aerospace transport [1]. Gliding and air breathing usually occur for hypersonic missiles. The hypersonic missiles of a scramjet or booster rocket are the latest international gun for striking [2]. The flight in the dive phase directly determines if the strike mission can be carried out [3] after the whole manoeuvring. Some researchers have actively tried to improve the performance of the flight. In order to avoid the removal of aerodynamic rudders under harsh heating conditions[4], a controlled mechanism called Moving Mass Control (MMS) was designed for re-entry vehicles A new configuration is proposed for internal mass movements for bank-to-turn (BTT) control in particular[5]. Furthermore, a higher order

sliding mode (HOSM) and a double layer adjustment algorithm [6] are proposed for this corresponding and unmatched disturbance. The non-recursive HOSM observator for the finite and fixed time is also investigated and improves performance in the final time compared to the recursive HOSM differentiator[7]. The design and strong robustness of the control unit were recently paid greater attention by researchers. There has been little research however in the dive phase of hypersonic missiles on optimization paths. In this article the fighting scene in which the hypersonic missile attacks the fixed target on the floor is taken into account. In the immersion phase, we aim for the best maneuverable path to break the enemy air defense system and maximize goal penetration. In order to create an optimum trajectory, Mehta et al. developed and manufactured an overhead model with a hypersonic missile that incorporates terminal needs in order to maximize target pull[8]. A HOSM controller is suggested on the basis of this study for the optimal path to be traced with great strength and precision[9]. Zhu et al. also simplified the hyper-sonic missile model and obtained a three-dimensional maneuvering path based on optimal control theory[10] with linearisation of feedback. The missile is not only intercepted in addition to the theory of motion camouflage but also proposed guidelines for the targeting of the land[11]. The above studies take place on the premise of normal flight and the importance of choosing a suitable manoeuvring form has been ignored. Unlike traditional ballistic missiles, high-speed geometric lift-to-drag missiles are normally designed[ 12]. The way in which the travel is maneuvered thus affects its performance. For example, the path taken by normal flight and by inverted flight differs greatly. Dynamic pressure, heating transfer rates and normal overload limit the hypersonic missiles in the dive phase. This report examines two typical forms of maneuvering, i.e. the normal and inverted flight, with the single aerodynamic shape of hypersonic missiles. The problem of trajectory optimization consists of two main types, i.e. indirect methods and direct methods. When path constraints are taken into account by indirect methods, the design of an optimum trajectory becomes complex. The limit on the nominal overcharge was converted to the Euler angle limits, and the path was nullified by the angular view line (LOS) rate [13].[ 13]. This challenge to be addressed.

One disadvantage of the above study is that only the maxima of nominal extra charge is regarded and a further disadvantage is the relative straightness of the course achieved by the zeroing of the angle LOS rate, leading to low target penetration. The direct approach is widely used to solve the issue of path optimization to prevent the problem of analytical expressions from deriving. The optimal continuous time check is transformed by discrete and parametric time states and control to be a nonlinear programming (NLP) problem with finite dimensions. The key question is to develop and converge an algorithm rapidly. Many studies focused recently on developing algorithms for NLP resolution. In [24] an ideal path is introduced to achieve the genetic algorithm (GA) for the hypercarrier during the power-free swing phase and in the indirect method, the problem of initial value sensitivity is resolved. GA is also used to maximize the booster range in the hypersonic booster trajectory [15]. A semi-analytical algorithm is proposed and its performance shows that the accuracy of the computational computer is significantly higher than GA [16]. An algorithm for pattern search (PS) has also been developed in order to optimize the path of the boost glide hypersonic cars [17]. As a PS control parameter the lift to drag ratio ( $L/D$ ) was chosen and shown to be more effective than GA. In the upward phase optimization of the path of multi-combined cycle engine vehicles [18] is also used with the particulate swarm optimizing algorithm (PSO), as well as the hyper-per-sonic weapons re-enter phase [20].

## II. THE GAUSS PSEUDO SPECTRAL METHOD

It was widely used in solving trajectory problems, a direct method. GPM for the hypersonic vehicle return phase [22], mid-speed interception phase [23] and the ascent phase of ramjet vehicles [22] are all achieved to achieve optimal trajectories [24]. Moreover, with the Turbine Combined Cycle engine GPM can help optimize trajectories in supersonic vehicles [25]. In comparison with other direct methods, the advantage of GPM is that the Karush Kuhn Tucker (KKT) transformed NLP conditions are compatible with the optimum conditions of the first-order control problem, which is continually optimized [26]. In addition, GPM provides an optimal global treatment for complex issues and is promising. GPM is therefore a good option to solve the trajectory optimization problem in this paper. To achieve better performance, the GPM must be improved. In [27], a pH meshing method is presented in order to reduce calculation and ensure accuracy. Consequently a hp-adaptive pseudo spectral approach [27] can be used to complete a temporary detection mission [28] to ensure the optimal path of a spatial plane in the re-entry stage. The weakness of the mesh [27] is that the mesh is only able to increase in size, thus increasing its calculation burden. To further optimize the

algorithm, the adaptive mesh refining processes with mesh size decrease are studied [29]. The mesh refinement algorithm was developed [30] in the last study. Thus, for a solution of the optimized trajectory issue for hypersonic dive rockets the improved PST method is introduced.

The literatures referred to above are based on an optimized pseudo-spectral method for hysterical missiles and provide the optimal manoeuvring path for the dive. First and foremost is the aerodynamically realistic and comprehensive NASA data model for the hyperbolic missile [31]. Then the maneuvering form of the hypersonic missile is discussed. It must be noted that the value of the inert angle (AoO, in its Spanish initials) is set as the corner of the normal surface and missile path [8]). The value of the AoO is linked to this. In particular, this paper adopts a strategy to maneuver inverted flight. The flight can use the lift for a larger path angle (i.e. a smaller AoO) to switch the direction of speed at the speed of hit. A pre-defined angle of flight terminal is then designed to reduce attack time, taking account of angle, dynamic pressure, warming rate and normal overload restrictions. An algorithm is also presented using an improved pseudo spectral hp adaptive method to solve the optimization problem that has been developed. This document has main contributions: To achieve an optimal maneuvering track, an advanced end to the terminal flight path is planned. The maneuvered flight shape is chosen in particular. An improved HP-adaptive pseudo spectral method with mesh size reduction is presented to solve the designed trajectory optimization problem.

The rest of the article is arranged accordingly. The following section provides the model and describes an optimal maneuvering flight path by inverted flight. The third part gives the detailed solution algorithm for the maneuvering path designed. Sections four and five present a simulation of numbers and a conclusion

## III. HYPERSONIC MISSILE MODEL

The following is the description of the kinematical and dynamic equations of the hypersonic missiles in the ground coordination system, ignoring earth rotation and assuming the earth is a sphere [32].

This article is based on current NASA [31] data and the aerodynamic model used in this document. The lower square error criterion and quasi-Method modified by Newton in [33] are the smallest residual between the fitting curve and the actual data compared with non-linear curve fitting processes in [35][36]. The purpose of this article is thus to adopt the Curve Fitting Model [33]. The terms CL, CD and CN are set out in the Appendix.

$$\begin{aligned}
 \dot{x} &= V \cos \gamma \cos \psi \\
 \dot{h} &= V \sin \gamma \\
 \dot{z} &= -V \cos \gamma \sin \psi \\
 \dot{V} &= \frac{-D}{m} - g \sin \gamma \\
 \dot{\gamma} &= \frac{L \cos \sigma - N \sin \sigma}{mV} - \frac{g}{V} \cos \gamma \\
 \dot{\psi} &= -\frac{L \sin \sigma + N \cos \sigma}{mV \cos \gamma}
 \end{aligned} \tag{1}$$

The position vector of the hypersonic missile is components of  $x$ ,  $h$ , and  $z$ .  $V$ ,  $\beta$ , and  $\psi$  indicate respectively the speed, the angle of flight path and the angle of heading. The angle of the bank.  $m$  is the weight of the vehicle, and  $g$  is the speed of gravity. The elevator  $L$ , drag  $D$ , and the side force  $N$  are provided as

$$\begin{aligned}
 L &= qSC_L \\
 D &= qSC_D \\
 \{N &= qSC_N \\
 q &= \frac{1}{2} \rho V^2, \quad \rho = \rho_0 \exp\left(\frac{h_0 - h}{h_s}\right)
 \end{aligned} \tag{2}$$

Where  $q$  is the dynamic pressure and  $S$  is the reference zone. The air density – air density and model  $\dot{S}_0$ ,  $h_s$ [34] of the atmosphere are constant. The elevator, drag and lateral force coefficient are indicated by  $C_L$ ,  $C_D$ , and  $C_N$ . Description this paper takes account of the scene in which a hypersonic missile attacks the target.

**A. Trajectory Optimization Description**

The path in diving is essential to the success of the strike mission during the entire strike mission because it directly determines whether the air defense system can be interrupted by hypersonic missiles, causing effective damage to the target. Hypersonic missiles are disrupting and deploying speed through the enemy's air defense system to prevent side operation. First of all, two typical maneuvers study the normal flight and the inverted flight. The diagrams for schematic strength analysis are presented in two maneuvers in figure. 1.

In addition, the centripetal acceleration  $a_C$  is expected to be large enough to provide a smaller AoO that improves its damage potential. The greater the  $a_C / a_T$  value, the more advantageous it will be for the flight without regard to the constraints. It can be concluded that

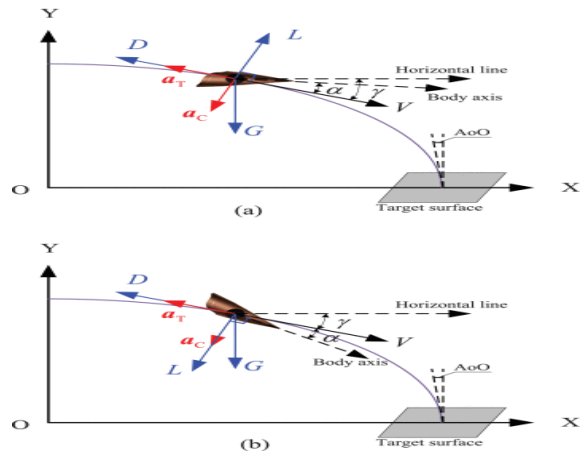


Fig. 1. Schematic force analysis diagrams in two forms. A) Use of the flight as normal. B) inverted flight use. The centripetal acceleration  $C$  and the tangential acceleration  $T$  are shown as follows by an analysis of the forces of this missile.

$$\begin{aligned}
 a_C &= \frac{G \cos \gamma \pm L}{m} \\
 a_T &= \frac{D - G \sin \gamma}{m}
 \end{aligned} \tag{3}$$

Where gravity is indicated by  $G = mg$ . For normal or reverse flights, the " $\pm$ " symbol will be selected as "-" or as "+". The shortest attack time is required to reduce the response time of the air defense system. The shorter the time you fly, the less the loss of cinematic energy. The tangential acceleration  $a_T$  should therefore be sufficiently small to remain a great value for the velocity.

For normal flight, the angle attack (AoA) must be negative if the value of  $a_C$  is to be great. At this time, it will be difficult to design the control system. The above problems are avoided by using the inverted flight. In addition,  $L/D$  features better in inverted flight than those in normal flight, resulting in a higher  $a_C / a_T$  value. The reverse flight therefore has further advantages in the dive phase of the hypersonic missile.

By minimizing costs, the manoeuvring trajectory objectives are selected

$$J = \phi(X(t_0), t_0, X(t_f), t_f) = t_f \tag{4}$$

Under the dynamic restriction

$$\dot{X} = f(X(t), u(t), t) \tag{5}$$

Under the the terminal state constraint

$$\phi = [x - x_f, h - h_f, z - z_f, \gamma - \gamma_f]^T = 0 \tag{6}$$

Under the the control constraints

$$\alpha_{min} \leq \alpha \leq \alpha_{max}, \beta = 0 \tag{7}$$

And the constraints

$$\begin{cases} q \leq q_{max} \\ Q_{rate} = C\rho^{0.5}V^{3.07}q_{\alpha} \leq \{Q_{rate}\}_{max} \\ q_{\alpha} = h_0 + h_1\alpha + h_2\alpha^2 + h_3\alpha^3 \\ |n_y| = |(L\cos\alpha + D\sin\alpha)/(mg)| \leq \{n_y\}_{max} \end{cases} \tag{8}$$

Where  $X(t)=[x, h, z, V, \gamma]^T$ , and the  $u(t)=[\alpha, \beta, \gamma]^T$ .  $J$  is the index criterion, and  $f$  is the final value of the variables. The same applies. (11) Eqs is derived. (1)~[6].  $Q_{rate}$  is the transmission rate of heating, and  $n_y$  is the usual missile overload. Eq's parameters. [23],[ 37]: $C=9.28$  checked by: $= 9.29$  checked by the following:  $h_2=0.6988$  checked by the newsletter[ 24.2 checked].

**IV. DESIGN OF THE ALGORITHM**

An hp-adaptive pseudospectral method to solve the path optimization question described under Eqs has been introduced in this section. (2)~ (27). (3) First of all, the problem of trajectory optimisation becomes the discernible bolza problem in a mesh  $M$ . Then, the transformed NLP problem is solved by a mesh refinement method. In contrast to the traditional pseudospectral hp-adaptive method, the mesh scale can be reduced by reducing the number of colloquial points and fusion of adjacent mesh intervals. Finally, the algorithm is summarized for the problem of trajectory optimization.

The trajectory optimization for the hypersonic missiles at dive is a problem of non-smooth optimization under various constraints. Bolza Optimum Control Problem The description in analytical form is very complex when we use an indirect method for resolving this problem. The GPM is happily an effective way of dealing with multiple limitations for the optimal problem. The drawback of GPM is that the number of discrete points must be increased, which reduces computational speeds. An hp-adaptive strategy [21] which improves performance by dividing up the time interval into several sub-intervals is often employed to address the

demand for solution accuracy and convergence speed in order to overcome the above disadvantage. We initially transform the path optimization described as Eqs to facilitate the description of a mesh refinement method in the latter section. (10)~(16) as an optimal control problem for discrete bolts.

The trajectory optimization issue time domain is  $[t_0, t_f]$ . But Gauss' pseudospectral techniques distribute the discrete points in  $[-1, +1]$ . The interval  $t$  for  $[t_0, t_f]$  is thus first transformed to the interval  $[-1, +1]$ . This is done in the first place. Assume the time  $\mu$   $[-1, +1]$  is divided into a mesh of intervals of  $K$  mesh

$$\begin{aligned} S_k &= [T_{k-1}, T_k] \\ -1 &= T_0 < T_1 < \dots < T_k = +1 \end{aligned} \tag{9}$$

$$\bigcup_{k=1}^K S_k = [-1, +1] \tag{10}$$

$K=1, \dots, K$ .  $K=1, \dots$  The continuous-time  $X^{(k)}(\beta)$  and  $u^{(k)}(\tau_i)$  inputs in  $S_k$  are approximated to  $\bar{X}^{(k)}(\hat{n})$  and  $\bar{u}^{(k)}(\hat{n})$  respectively by introducing the collocation points  $N_k$  Legendre-Jauss-Radau (LGR). The optimisation of the path is described as Eqs. (10)~(16) shall be re-written accordingly. Reduce the functional costs

$$J = \phi(\bar{X}_1^{(1)}, t_0, \bar{X}_{N_K+1}^{(K)}, t_f) = t_f \tag{11}$$

Under the dynamic constraint

$$\sum_{j=1}^{N_k+1} D_{ij}^{(k)} \bar{X}_j^{(k)} = \frac{t_f - t_0}{2} f(\bar{X}_i^{(k)}, \bar{U}_i^{(k)}, t(\tau_i^{(k)}, t_0, t_f)), \quad i = 1, \dots, N_k$$

Under the path constraints

$$C(\bar{X}_i^{(k)}, \bar{U}_i^{(k)}, t(\tau_i^{(k)}, t_0, t_f)) \leq 0, i = 1, \dots, N_k$$

and Under the boundary condition

$$\psi(\bar{X}_1^{(1)}, t_0, \bar{X}_{N_K+1}^{(K)}, t_f) = 0 \tag{12}$$



Where the path limitations are the limitations described as Eqs. (13)~ (16) And Eq is equivalent to the limiting condition. D (k) in is the component of the LGR differentiation matrix Nk pour (Nk+1) [38]. The algorithm is summarized as follows to resolve the problem of trajectory optimization.

Transform the problem described as Eqs in trajectory optimization. (10)~ (16) Into bolza as described as Eqs, an optimal control problem. (18)~ (19).

The initial mesh m includes the K mesh intervals  $S_k=[T_{k-1}, T_k], k=1, \dots, K, N_k$  with  $S_k$ .

Solve the problem described as Eqs of bolza optimal control. (17)~ (20) in[ 39] using the SNOPT NLP solver.

The Eq estimates the relative maximum error  $e(k)_{max}, k=1, \dots, K$ , at present mesh M. 22].

If  $e_{max} \wedge (k)$  unfairness holds all  $k=1, \dots, K$ , stops.

Continue to step 6 otherwise. Get an M+1 mesh sophisticated. For every mesh interviewing,  $S_k=[T(k-1), T k], k=1, \dots, K, (a)$  when the tolerance of error is not met; i.e.,  $e(k)_{max} > \epsilon'$ , divide the mesh interval (by Eq. (24)). (b) If the mistake limit is met, i.e. the amount of colloquial nodes and neighbouring panel ranges are decreased.

V. SIMULATIONS

This chapter performs a simulation research to examine the efficiency of this paper's optimal maneuvering path. Three elements of the simulation are conducted. First, contrasting the pseudo-spectral approach[ 27] verifies the findings of the enhanced pseudo-adaptive hp-spectral technique proposed for this document. Secondly, a vibrant system as outlined in Eqs is to be solved by Runge-Kutta in order for the path acquired through the constructed engine to be checked in accordance with the aircraft legislation. Also with the proposed matrix Section III, the Runge-Kutta technique will fix the optimization problem. (1)~(6) The finest trajectory for the entry device. Finally, the reversed aircraft effectiveness is evaluated by contrasting the normal and reversed flight outcomes.

A. Method of refining mesh results result

The hypersensitive optimal control problem [40] is considered to assess the performance of the mesh refinement method suggested in Section III. The aim is chosen through a reduction of costs

$$J = \frac{1}{2} \int_0^{t_f} (x^2 + u^2) dt$$

Subject to the dynamic

constraint,  $\dot{x} = -x + u$  and the boundary conditions

$$x(0) = 1.5, x(t_f) = 1$$

Where  $t_f$  is fixed. The parameter M is the number of mesh raff nations, and M=0 is the initialization of the mesh. The fixed terminal time  $t_f$  is selected as 10000 because of the Eqs solution. (31)~ (33) shows a so-called departure, cruise and landing structure with a sufficiently large  $t_f$ . The initial mesh M=0 consists of 10 mesh intervals evenly distributed, and 2 mesh collocation points. The tolerance of the error  $\mu=10^{-6}$ . The results of the simulation are shown in figures. (2)~ [3].

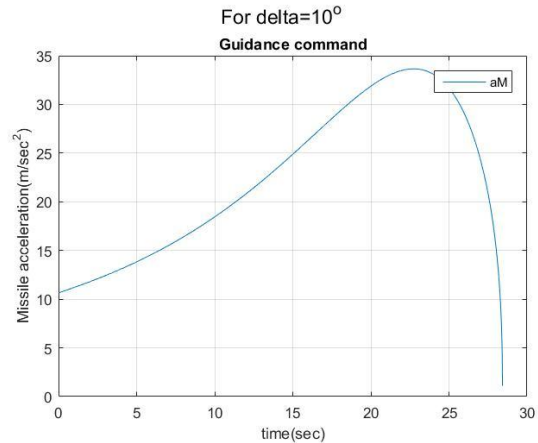


Fig. 2. Exact solution with  $t_f=10000$  to the hypersensitive issue (a) State against time. State vs. (b) Time vs. control

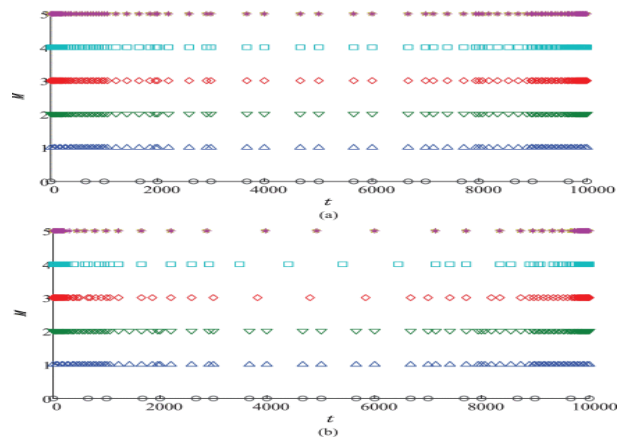


Fig. 3. The error tolerance  $\mu=10^{-6}$  mesh refining history. (a) Mesh history of refining by the procedure in [27]. (b) The history of mesh refining by the method proposed;

B. Results of Optimal Trajectory

Model parameters of the hypersonic missile are set to[ 33] and atmosphere model parameters[ 34] are chosen as "sluges" for "Sluges,"  $\alpha(-3), h_0=85000$  ft,  $h_s=21,358$  ft.[ 32] The parameters in the atmospheric

missile are selected[ 33] This is the original status of  $x_0=0$   $h_0=85000$  ft,  $V_0=7700$ ft / s,  $\mu_0=0$ .  $x_f=4$  to 105 ft  $h_f=0$  to  $\mu_f$   $f=-z_u$  65 to  $\mu_o$ , "the end state limitations are given. The following are the maximum values of dynamic pressure, heat transfer rates and normal overload:

$$q_{max} = 3.1315 \times 10^4 \text{ lbF}/(\text{ft}^2)$$

$$\{n_y\}_{max} = 10, \{Q_{rate}\}_{max} = \frac{200 \text{ BTU}}{\text{ft}^2 \cdot \text{s}}$$

form is chosen as an inverted flight. Since the pseudo spectral Gauss-Adaptive methods obtain a status approximation by polynomial interpolation from Gauss-Lobito, rather than by numerical integration, the results of optimization algorithms must be compared to the numerical integration results. The  $\alpha$  control of the optimal path is considered to be the input for the Eqs model difference equations. (1)-(6) and the Runge-Kutta method results for numerical integration. The results of the simulation are shown in figures. (4)- [2].

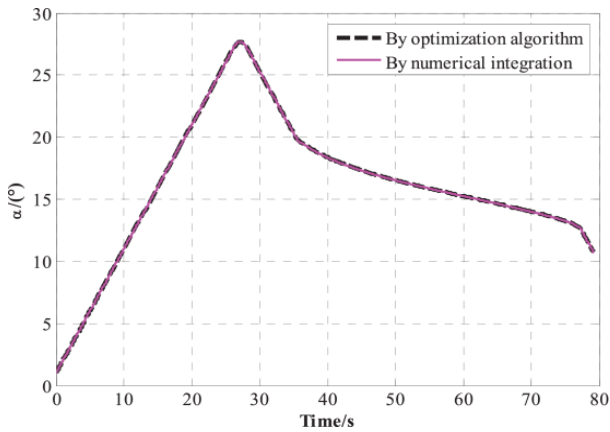


Fig. 4. Curves of the angle of attack

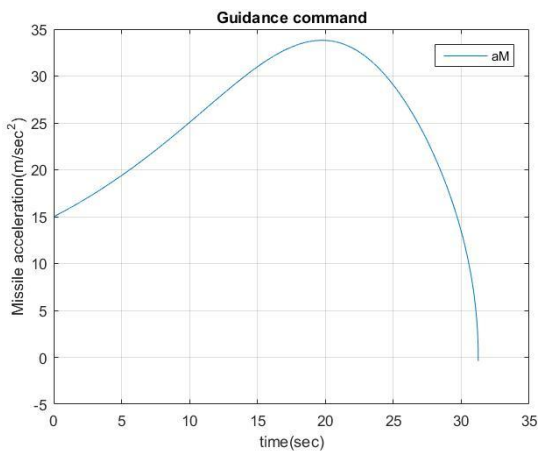


Fig. 5. Curves of the trajectory.

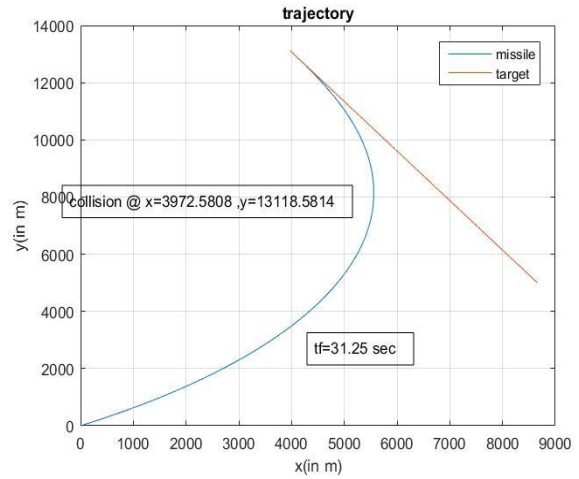


Fig.6. Curves of the velocity.

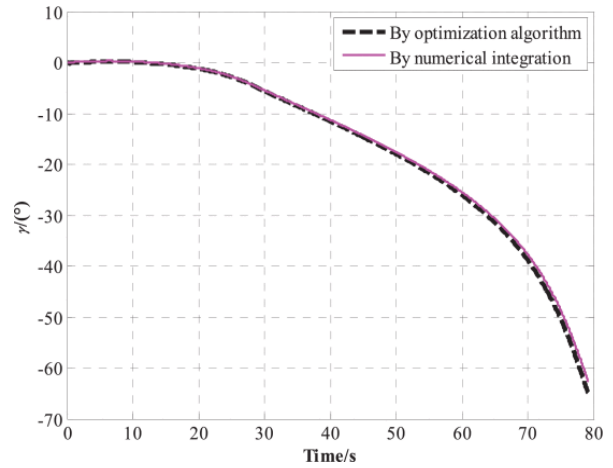


Fig. 7. Curves of the flight path angle.

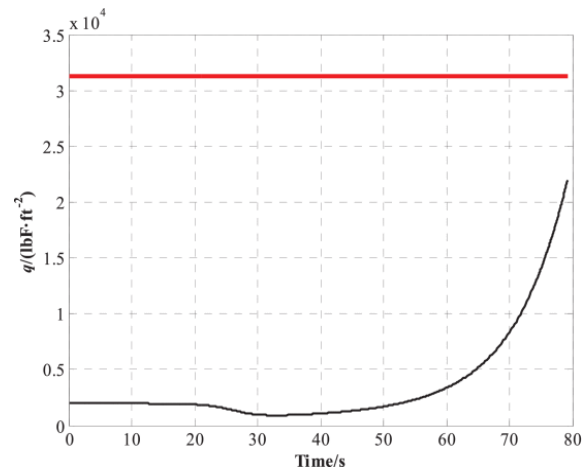


Fig. 8 Curve of the dynamic pressure.

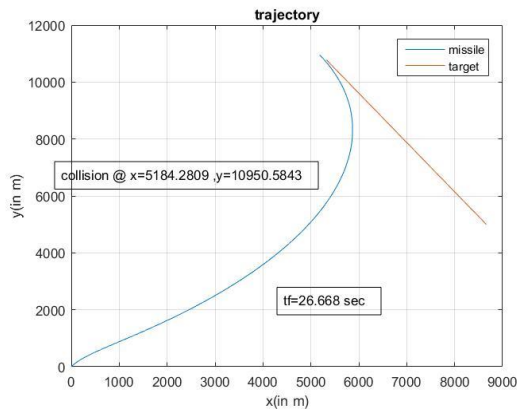


Fig. 9. Curve of the heating transfer rate.

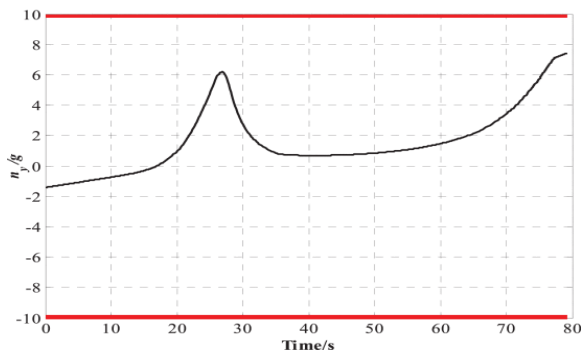


Fig. 10. Normal surcharge curve.

Figs. (4)~ (7) show the angles, the trajectory, the speed and the angles of the airway. The results of the proposed optimization algorithm are shown as pointed lines and results are shown as solid lines through numerical integration. In contrast to this, the results are consistent with those of numerical integration in the proposed trajectory optimization algorithm. The proposed optimization algorithm can be concluded to reflect with a high precision the actual motion law of the hypersonic missile. In addition, the results indicate that the entire path of manoeuvring is smooth.

Next, we analyse the trajectory characteristics achieved by the proposed algorithm for trajectory optimisation. As Fig shows. In a reasonable range,  $\alpha$  dais (0, 30 bus koi's) is the control input, i.e. the angle of attack. In the picture. (5), the optimum manoeuvring path suggests that the target location of the hypersonic missile is reached. It is visible from Fig. (6) That the rate is a downward trend caused by heating and dynamic pressure constraints. Fig.-Fig. (7) shows a pre-set value for the terminal flight path angle. Figs.-Figs. (8)~ (10) show the dynamic pressure curves, heat transfer rate and normal overload. The results show that during the entire flight, dynamic pressure, transmission rates and normal surge are within their constraints.

## VI. COMPARISON OF NORMAL FLIGHT AND INVERTED FLIGHT

The following simulation is carried out in order to assess the efficiency of the inverted flight. Table 1 selects the manoeuvring form and the flight path angle and other conditions are the same as in Section B. The results of the simulation are shown in Fig. (10)~ (25).

TABLE 1 Flight Path Angles manipulation of forms and terminal

Trajectory number	Maneuvering form	Constraint of terminal flight path angle
Tra 1	Normal flight	35°
Tra 2	Normal flight	50°
Tra 3	Normal flight	65°
Tra 4	Inverted flight	35°
Tra 5	Inverted flight	65°
Tra 6	Inverted flight	80°

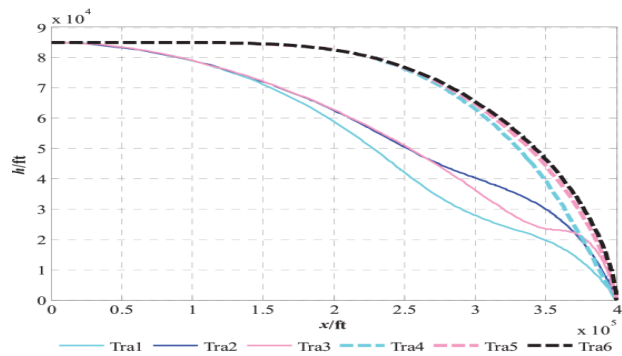


Fig. 11. Curves of the trajectory.

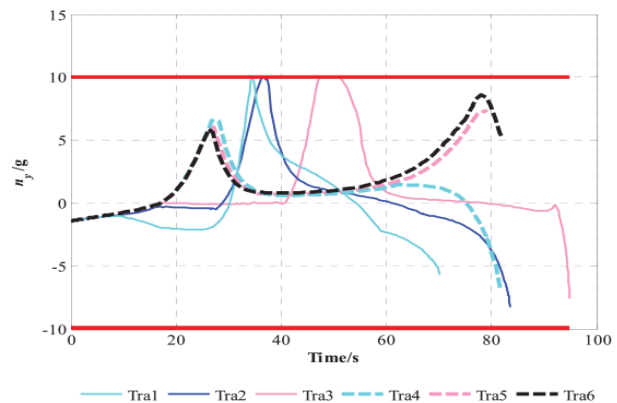


Fig. 12. Curves of the normal overload.

Picture. (11) shows Tra 1~Tra 6 path curves. The inverted flight path curve is approx. parabola in shape and is smoother than normal flight. It may be shown. During the simulation process, we found an optimum trajectory within a large terminal flight path angle

with inverted flight was relatively easy to achieve. But a large predetermined terminal fl

## VII. CONCLUSION

The hyper-persona missiles in the dive phase in this paper are presented with an optimum manoeuvre. Compared to earlier studies, hypersonic missiles first have a manoeuvring form called the inverted flight. In addition, the pseudo spectral method is designed to address the trajectory optimization problem with an improved PS-adaptable method with mesh size reduction. Simulation results indicate that the proposed algorithm can reduce the mesh size significantly with a satisfactory precision, and comparative simulation checks the effectiveness of the inverted flight. The paper offers a strategy of manoeuvre for hypersonic missiles in the dive phase to break the enemy's air defense system and maximize the penetration target.

## REFERENCES

- [1] J. Breckling, Ed., *The Analysis of Directional Time Series: Applications to Wind Speed and Direction*, ser. Lecture Notes in Statistics. Berlin, Germany: Springer, 1989, vol. 61.
- [2] S. Zhang, C. Zhu, J. K. O. Sin, and P. K. T. Mok, "A novel ultrathin elevated channel low-temperature poly-Si TFT," *IEEE Electron Device Lett.*, vol. 20, pp. 569–571, Nov. 1999.
- [3] Umakant B. Gohatre, Venkat P. Patil, "Performance analysis of Novel Technique for Video Based Real Time Object Detection in 2 Dimensional and 3 Dimensional Visual System" *IJECS*, Volume 6, Issue 9, ISSN 2348-117X, September 2017
- [4] M. Wegmuller, J. P. von der Weid, P. Oberson, and N. Gisin, "High resolution fiber distributed measurements with coherent OFDR," in *Proc. ECOC'00*, 2000, paper 11.3.4, p. 109.
- [5] R. E. Sorace, V. S. Reinhardt, and S. A. Vaughn, "High-speed digital-to-RF converter," U.S. Patent 5 668 842, Sept. 16, 1997.
- [6] (2002) The IEEE website. [Online]. Available: <http://www.ieee.org/>
- [7] M. Shell. (2002) IEEEtran homepage on CTAN. [Online]. Available: <http://www.ctan.org/tex-archive/macros/latex/contrib/supported/IEEEtran/>
- [8] Umakant B. Gohatre, Venkat P. Patil "A Robust Approach towards Unknown Transformation, Regional Adjacency Graphs, Multigraph Matching, Segmentation Video Frames From Unnamed Aerial Vehicles (UAV)", International conference on Electrical, Electronics, Materials and Applied Science (ICEEMAS-2017), 22nd and 23rd December 2017, Organized by Swami Vivekananda Institute of Technology, Secunderabad, Telangana, India
- [9] FLEXChip Signal Processor (MC68175/D), Motorola, 1996.
- [10] "PDCA12-70 data sheet," Opto Speed SA, Mezzovico, Switzerland.
- [11] A. Karnik, "Performance of TCP congestion control with rate feedback: TCP/ABR and rate adaptive TCP/IP," M. Eng. thesis, Indian Institute of Science, Bangalore, India, Jan. 1999.
- [12] Umakant B. Gohatre, Venkat P. Patil, Chetan Patil, "Performance Evaluation of Feature Types For Object Detection and Classification", *International Journal of Management, Technology And Engineering* Volume 8, Issue X, OCTOBER/2018 ISSN NO : 2249-7455, Page 1377
- [13] J. Padhye, V. Firoiu, and D. Towsley, "A stochastic model of TCP Reno congestion avoidance and control," *Univ. of Massachusetts, Amherst, MA, CMPSCI Tech. Rep.* 99-02, 1999.
- [14] *Wireless LAN Medium Access Control (MAC) and Physical Layer (PHY) Specification*, IEEE Std. 802.11, 1997.